J. Resour. Ecol. 2021 12(5): 609-619
DOI: 10.5814/j.issn.1674-764x.2021.05.004
www.jorae.cn

Spatio-temporal Pattern of Surface Albedo in Beijing and Its Driving Factors based on Geographical Detectors

LIU Qinqin[1, 2], TIAN Yichen[2], YIN Kai[2], ZHANG Feifei[2], YUAN Chao[2], YANG Guang[2,*]

1. University of Chinese Academy of Sciences, Beijing 100049, China;
2. Aerospace Information Research Institute, Chinese Academy of Sciences, Beijing 100101, China

Abstract: Surface albedo directly affects the radiation balance and surface heat budget, and is a crucial variable in local and global climate research. In this study, the spatial and temporal distribution of the surface albedo is analysed for Beijing in 2015, and the corresponding individual and interactive driving forces of different explanatory factors are quantitatively assessed based on geographical detectors. The results show that surface albedo is high in the southeast and low in the northwest of Beijing, with the greatest change occurring in winter and the smallest change occurring in spring. The minimum and maximum annual surface albedo values occurred in autumn and winter, respectively, and showed significant spatial and temporal heterogeneity. LULC, NDVI, elevation, slope, temperature, and precipitation each had a significant influence on the spatial pattern of albedo, yielding explanatory power values of 0.537, 0.625, 0.512, 0.531, 0.515 and 0.190, respectively. Some explanatory factors have significant differences in influencing the spatial distribution of albedo, and there is significant interaction between them which shows the bivariate enhancement result. Among them, the interaction between LULC and NDVI was the strongest, with a *q*-statistic of 0.710, while the interaction between temperature and precipitation was the weakest, with a *q*-statistic of 0.531. The results of this study provide a scientific basis for understanding the spatial and temporal distribution characteristics of surface albedo in Beijing and the physical processes of energy modules in regional climate and land surface models.

Key words: albedo; spatio-temporal distribution; explanatory factors; geographical detectors

1 Introduction

Surface albedo is a non-dimensional parameter defined as a ratio of surface-reflected radiation to incident radiation (Ranson et al., 1991; Russell et al., 1997). It is one of the most critical parameters in surface energy budget studies, and its temporal and spatial changes are closely related to global climate change and regional weather systems (Dickinson, 1983; Richardson et al., 2013). Therefore, understanding the spatial and temporal distribution of surface albedo and its influencing factors can provide not only a powerful reference for simulating environmental climate change but also a theoretical basis for the parameterization of surface albedo models.

Surface albedo is usually determined by the land cover type and, as such, changes in land use can have strong influences on surface albedo (Bounoua et al., 2002; Liu et al., 2015; Liu et al., 2019). It is also affected by many factors, including solar elevation angle, surface roughness, normalized difference vegetation index (NDVI), meteorological factors, soil moisture, etc. (Govaerts et al., 2008; Loarie et al., 2011; Xiao et al., 2011; He et al., 2014). In previous studies, the linear regression method was usually used to analyze the correlations between surface albedo and driving factors (Yang et al., 2020). However, because of the com-

Received: 2021-01-08 **Accepted:** 2021-04-02
Foundation: The Major Project of High Resolution Earth Observation System (06-Y30F04-9001-2022); The National Natural Science Foundation of China (41471423).
First author: LIU Qinqin, E-mail: liuqinqin18@163.com
*__Corresponding author:__ YANG Guang, E-mail: yangguang201924@aircas.ac.cn

Citation: LIU Qinqin, TIAN Yichen, YIN Kai, et al. 2021. Spatio-temporal Pattern of Surface Albedo in Beijing and Its Driving Factors based on Geographical Detectors. *Journal of Resources and Ecology*, 12(5): 609–619.

plex process of the surface albedo responses to driving factors, the inflexible statistical linear models may not be able to accurately describe the internal relationships between the two variables. Spatial heterogeneity is a common feature of ecological geographical phenomena. Studies have shown that the spatio-temporal distribution of surface albedo display distinct geographical differences (Zhang et al., 2010; Nikolaos and Nektarios, 2015). The traditional linear analysis method usually only unifies the relationships between independent variables and dependent variables, and lacks the consideration of spatial heterogeneity of the variables. Geographical detectors are a set of statistical methods which can detect spatial stratified heterogeneity (SSH) and reveal the driving forces behind them. The central premise of these methods is the assumption that if the sum of the variances of the subregions is less than the total regional variances, then spatial differentiation exists. If an independent variable has an important influence on a dependent variable, the spatial distributions of the independent and dependent variables should be similar (Wang et al., 2010; Wang et al., 2016).

Geographical detectors were first used in health studies to determine the environmental factors associated with neural tube defects in new-borns and earthquake deaths (Liao et al., 2010; Hu et al., 2011; Wang et al., 2012). This approach can be used to measure and characterise the spatial heterogeneity of a target variable (Golkar et al., 2018; Malahlela et al., 2019), assess the degree of coupling between two variables, and investigate the interaction between two explanatory variables forced by a response variable (Yuan et al., 2019). Studies have applied geographical detectors to identify the driving factors of $PM_{2.5}$ pollution (Lou et al., 2016; Yang et al., 2018; Ding et al., 2019), the driving force analysis of the spatial and temporal distribution of urban expansion (Wang et al., 2019; Yan et al. 2020), the impact of new transportation modes on population distribution (Wang et al., 2018), and many other relationships. Factor detector and interaction detector were used to detect that cumulative temperature, soil salinity and their interactions were the key factors affecting winter wheat yield (Chu et al., 2019). The interaction detector has shown that the interaction between economic activities and the urban environment has the greatest influence on the temperature of the Yangtze River Delta region (Zhou et al., 2020). The stratification heterogeneity of traffic accidents in Shenzhen was found by using geographical detector, and the results of factor detector showed that the influencing factors of fatalities and injuries are different (Zhang et al., 2020).

Since 2010, geographical detectors have been increasingly used in studies of natural, humanistic, economic and other factors with spatial heterogeneity. However, the detection of factors affecting the distribution of surface albedo using geographical detectors remains limited. To address this gap, this study sought to analyse the spatio-temporal distribution of surface albedo in Beijing in 2015 using the Global Land Surface Satellite (GLASS) albedo products. Based on the geographical detectors approach, the following explanatory factors of surface albedo were detected: land use and land cover (LULC), NDVI, elevation, slope, average temperature, and cumulative precipitation. In this study, the quantitative relationship between surface albedo changes and their driving factors in Beijing were studied by using geographical detector. The contributions of different driving factors to surface albedo change were compared, and the correlations of driving factors in influencing surface albedo change were studied. The results provide not only a new method for studying the driving factors of surface albedo variability but also a reference for improving regional-scale climate and land-surface process simulations.

2 Materials and methods

2.1 Study area

Beijing, the capital of China, is the national centre of politics, culture, and scientific and technological innovation, is located in the north of China and the north of the North China Plain, at 39°54'20"N and 116°25'29"E (Fig. 1). The total area of Beijing is 16412 km^2, with a built-up area of 1485 km^2. The terrain of the city is high in the northwest and low in the southeast with the mountainous areas accounting for 62% of the total area and the remaining 38% consisting of flatter plains. The average elevation is 43.5 m, while the elevation of the plain is 20–60 m, and the elevation of the mountain is generally 1000–1500 m. Beijing's climate is a typical north temperate semi-humid continental monsoon climate, with a high temperature and rainy in summer, cold and dry in winter, and a short spring and autumn. The average annual sunshine hours in Beijing are between 2000 and 2800 hours and the annual average solar radiation is 112–136 kcal cm^{-2}. Therefore, Beijing is taken as the research area for the exploration of spatial heterogeneity and driving factors of surface albedo in this study.

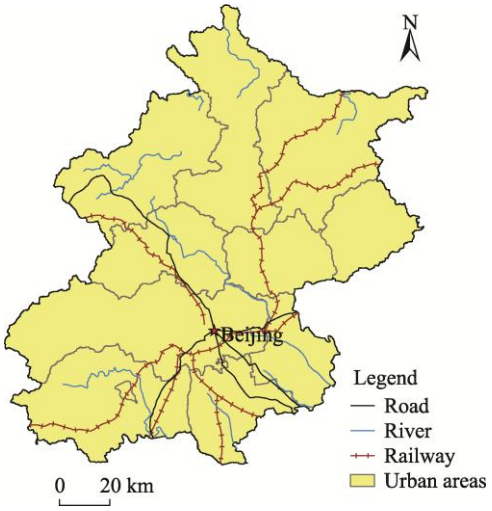

Fig. 1 Study area: Beijing, China.

2.2 Datasets

2.2.1 Surface albedo

Surface albedo data were obtained in the form of the Global Land Surface Satellite (GLASS) products from the National Earth System Science Data Sharing Infrastructure, National Science & Technology Infrastructure of China (http://www.geodata.cn) (Liu et al., 2013a; Liu et al., 2013b; Qu et al., 2014). These data have a 1-km spatial resolution and an eight-day temporal resolution. Compared to the Moderate Resolution Imaging Spectroradiometer (MODIS) MCD43 product, GLASS albedo products overcome the missing values resulting from snow-covered areas (Schaaf et al., 2002). By including black-sky albedo and white-sky albedo data, the GLASS albedo product has been widely favoured, and its level of precision can meet the needs of most surface albedo spatio-temporal analyses.

Data for 46 periods in 2015 were obtained as a total of 92 HDF files. The black-sky and white-sky albedo data were first extracted from each file and converted to an appropriate file format. A mosaic was then created for Beijing from two images acquired during the same period. Average black-sky and white-sky albedo values were then determined to quantitatively represent the surface albedo across the city. Finally, the average surface albedo during each period was determined along with the annual average (2015).

2.2.2 Explanatory factors

Land-use data for 2015 were acquired from the current Chinese Land-Use/Cover Datasets of Resource and Environment Data Cloud Platform (http://www.resdc.cn/) (Liu et al., 2014). The spatial resolution of land use data used in this study is 1 km, and the primary land-use classifications include cropland, forestland, grassland, water bodies, built-up land, and unused land. Figure 2a shows the distribution of land-use types and land covers in Beijing in 2015, which yields the following ranked order: forestland > cropland > built-up land > grassland > water body > unused land. Cropland and built-up land are mainly distributed in the southeast of the city, while forestland and grassland are mainly distributed in the northwest.

The Normalized Difference Vegetation Index (NDVI) products were the Terra Moderate Resolution Imaging Spectroradiometer (MODIS) Vegetation Indices (MOD13A3) obtained from the National Aeronautics and Space Administration (NASA). The data are provided monthly at 1km spatial resolution. In this study, the MODIS NDVI data for Beijing in 2015 were used to calculate its average to represent the characteristics of NDVI in Beijing. As shown in Fig. 2b, the NDVI of Beijing in 2015 is between 0.08–0.74, and the spatial distribution of NDVI in Beijing is quite similar to the spatial distribution of LULC. The NDVI of built-up land in the south-central part is the lowest, while the NDVI of grassland and forest land in the northwest is higher, and the NDVI of cropland is moderate.

A digital elevation model (DEM) of Beijing is available from the Geospatial Data Cloud Site, Computer Network Information Center, Chinese Academy of Sciences (http://www.gscloud.cn). These datasets were processed using the Advanced Spaceborne Thermal Emission and Reflection Radiometer Global Digital Elevation Model (ASTER GDEM V1), which is a digital elevation data product with a global spatial resolution of 30 m. The elevation map of Beijing is shown in Fig. 2c and spans an altitudinal range of between –129 m and 2270 m. Slope data for Beijing were generated from the DEM, which refers to the angle between the tangent plane passing through one point on the ground surface and the horizontal ground surface. A lower slope value indicates flatter terrain while a higher slope value indicates steeper terrain. The obtained slope values were categorised into five levels as shown in Fig. 2d.

Average temperature and cumulative precipitation data were acquired from the Resource and Environment Data Cloud Platform (http://www.resdc.cn/Default.aspx). The spatial interpolation database of annual temperature and precipitation data provided for China by the website is based on the daily observation data of more than 2400 meteorological stations in China, which is generated through sorting, calculation and spatial interpolation. The data for Beijing in 2015 were clipped using ArcGIS. The annual mean temperature of Beijing in 2015 ranged from 2.5 ℃ to 13.5 ℃, and annual total cumulative precipitation ranged from 534 mm to 630 mm. The spatial distribution of precipitation and rainfall are shown in Fig. 2e and Fig. 2f, respectively.

When exploring the relationships between independent variables and dependent variables, the geographical detector requires that the independent variables should be discrete data. If the independent variables are continuous data, they need to be discretized. Data discretization is the process of dividing continuous data into several intervals, where each interval corresponds to a qualitative symbol. The discretization can be based on expert knowledge or classified using algorithms such as k-means. User-defined discretization can also be used for geographical detector models (Wang et al., 2010; Hu et al., 2011; Cao et al., 2013). The explanatory factors in this study are all continuous data except for the LULC, therefore, the remaining five variables needed to be discretized. As shown in Table 1, the NDVI is discretized into six intervals: N1(0.08–0.30), N2(0.30–0.37), N3(0.37–0.44), N4(0.44–0.50), N5(0.50–0.56), N6(0.56–0.74); The elevation is discretized into six intervals: E1(–129–158 m), E2(158–389 m), E3(389–617 m), E4(617–854 m), E5 (854–1187 m), E6 (1187–2270 m); The slope is discretized

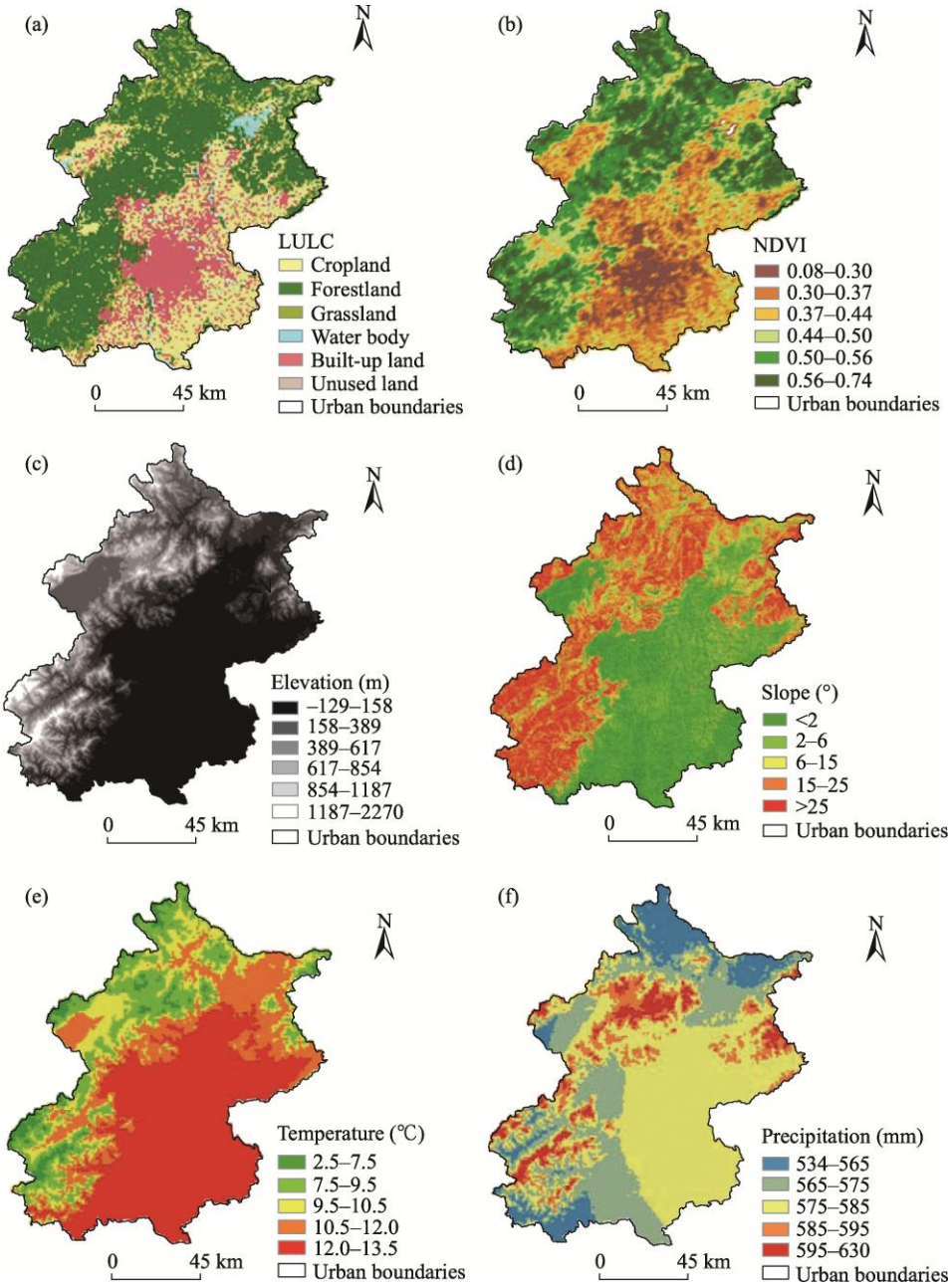

Fig. 2 Explanatory factor classification maps for (a) land use and land cover (LULC); (b) NDVI; (c) elevation; (d) slope; (e) annual mean temperature; and (f) annual cumulative precipitation.

Table 1 Discretization results of explanatory factors

Factors	NDVI		Elevation		Slope		Temperature		Precipitation	
	Values	Types	Values (m)	Types	Values (°)	Types	Values (℃)	Types	Values (mm)	Types
1	0.08–0.30	N1	–129–158	E1	<2	I	2.5–7.5	T1	534–565	C1
2	0.30–0.37	N2	158–389	E2	2–6	II	7.5–9.5	T2	565–575	C2
3	0.37–0.44	N3	389–617	E3	6–15	III	9.5–10.5	T3	575–585	C3
4	0.44–0.50	N4	617–854	E4	15–25	IV	10.5–12.0	T4	585–595	C4
5	0.50–0.56	N5	854–1187	E5	>25	V	12.0–13.5	T5	595–630	C5
6	0.56–0.74	N6	1187–2270	E6	–	–	–	–	–	–

Note: "–" means that the data is only divided into five categories.

into five intervals: I (<2°), II (2°–6°), III (6°–15°), IV (15°–25°), V(>25°); The temperature is discretized into five intervals: T1(2.5–7.5 ℃), T2(7.5–9.5 ℃), T3(9.5–10.5 ℃), T4(10.5–12 ℃), T5(12–13.5 ℃); And the precipitation is discretized into five intervals: C1 (534–565 mm), C2 (565–575 mm), C3 (575–585 mm), C4 (585–595 mm), C5 (595–630 mm). The slope is discretized based on expert knowledge, while NDVI, elevation, temperature and precipitation are discretized according to the actual values of each factor in Beijing.

2.3 Methods

Geographical detector is a novel tool for the measurement and attribution of SSH. It includes four detectors: factor detector, risk detector, ecological detector and interaction detector. In this study, geographical detectors were used to determine the influence of the explanatory factors outlined in Section 2.2.2 (LULC, NDVI, elevation, slope, average temperature, and cumulative precipitation) on the spatial pattern of surface albedo in Beijing. The factor detector, ecological detector, and interaction detector were applied as follows.

2.3.1 Factor detector

The factor detector mainly measures the SSH of variable *Y*, or the influencing power of an explanatory variable *X* on *Y*. Therefore, the power of the determinant of the explanatory factors of albedo can be measured by the *q*-statistic of factor detector by the following method (Wang et al., 2010):

$$q = 1 - \frac{\sum_{k=1}^{n} N_k \sigma_k^2}{N\sigma^2} \quad (1)$$

where N and σ^2 stand for the number of units and the variance of surface albedo in a study area, respectively; the population surface albedo is composed of n strata (k = 1, 2, ⋯, n) divided by the explanatory factors, N_k and σ_k^2 stand for the number of units and the variance of surface albedo in stratum k, respectively. The value of q is within [0, 1], and q = 0 indicates that there is no coupling between surface albedo and the explanatory factors, while q = 1 indicates that the surface albedo is completely determined by the explanatory factors.

2.3.2 Ecological detector

The ecological detector identifies the difference in the impacts of two explanatory variables and is measured by the *F* statistic (Wang et al., 2010):

$$F = \frac{N_{x_1}\left(N_{x_2} - 1\right)\sigma_{x_1}^2}{N_{x_2}\left(N_{x_1} - 1\right)\sigma_{x_2}^2} \quad (2)$$

where N_{x_1} and N_{x_2} are the numbers of units of the two explanatory factors, and $\sigma_{x_1}^2$ and $\sigma_{x_2}^2$ are the population dispersion variances of the two factors, respectively, where the null hypothesis is $H_0 : \sigma_{x_1}^2 = \sigma_{x_2}^2$. If the null hypothesis is rejected at the significance level, then two factors are considered to have significantly different effects on the spatial distribution of surface albedo.

2.3.3 Interaction detector

The interaction detector can be used to identify the interactions between different explanatory factors on the spatial distribution of the dependent variable. This detector compares the interaction between two factors A and B on the surface albedo, and determines whether the two determinants when taken together weaken or enhance each another, or are independent in affecting the surface albedo. This relationship evaluation method involves comparing $q(A)$, $q(B)$, and $q(A \cap B)$ and includes weakening, independent, and enhanced relationships, with the five relationships shown in Table 2 (Wang et al., 2012). Therefore, the interaction results not only indicate the contributions of the two factors to surface albedo, but also reveal whether there is co-linearity between the two factors.

Table 2 Types of interactions between two covariates

	Description	Interaction
1	$q(A \cap B) < \min(q(A), q(B))$	Weaken, nonlinear
2	$\min(q(A), q(B)) < q(A \cap B) < \max(q(A), q(B))$	Weaken, univariate
3	$q(A \cap B) > \max(q(A), q(B))$	Enhance, bivariate
4	$q(A \cap B) = q(A) + q(B)$	Independent
5	$q(A \cap B) > q(A) + q(B)$	Enhance, nonlinear

3 Results

3.1 Spatio-temporal variation of surface albedo in Beijing, 2015

Annual average surface albedo can be used to characterise the overall albedo of a region. The average surface albedo of 46 periods was calculated to represent the surface albedo of Beijing. Based on Fig. 3, the annual average surface albedo in Beijing varied between 0.050 and 0.196 in 2015 and showed marked spatial variation; values were relatively high in the southeast of the city (0.14–0.18) and relatively low in the northwest (0.05–0.14). The surface albedo of most regions was between 0.10 and 0.18, and the maximum (0.18–0.20) or minimum (0.05–0.10) surface albedo only occupied a small part of the region. As shown in Fig. 3, the spatial distribution of surface albedo is roughly similar to that of LULC, but there are differences. That is, the surface albedo of given land use type is not exactly the same and may show significant variations even within the same land-use category. For example, the surface albedo of an area of built-up land in the south-central region of the city was notably lower than the surrounding land of the same cover type. This indicates that the surface albedo is not only

determined by the type of land use, but is also affected by many other factors. For example, such as, in the case of built-up land, the likely results from the differences in the types of buildings or other factors.

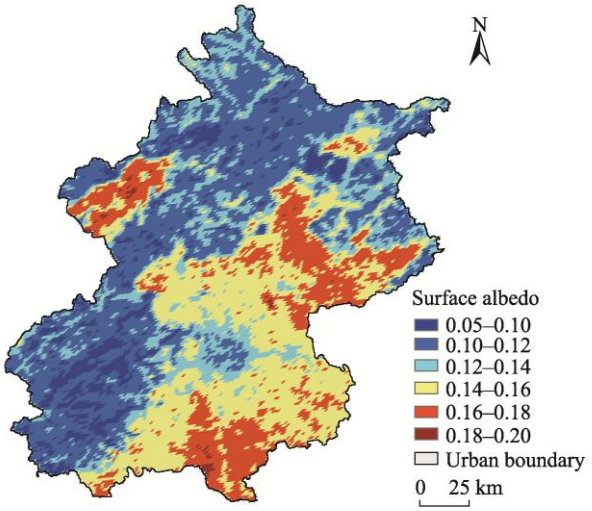

Fig. 3 Spatial pattern of annually averaged surface albedo in Beijing, 2015.

The average surface albedo across the whole region was determined as a representative value for the entire city. The average daily surface albedo of Beijing (as a whole) in 2015 varied between 0.114 and 0.227, with a mean of 0.131. As shown in Table 3, the seasonal averages of surface albedo of Beijing in 2015 are ranked in the following order: autumn (0.122) < spring (0.127) < summer (0.134) < winter (0.142), indicating that the surface albedo is the lowest in autumn and the highest in winter. Combining these results with Fig. 4, the smallest variability occurred in spring, remaining at approximately 0.127 (day 30–120), but rising slightly towards the beginning of summer to reach 0.136. A slight decrease in variability occurred during the middle and late summer (day 145–210) and a more marked decline occurred during the autumn (day 210–300) reaching a minimum of 0.114. Variation was greatest during the winter (day 300–30 of the next year), reaching a significant peak of 0.227 on day 329.

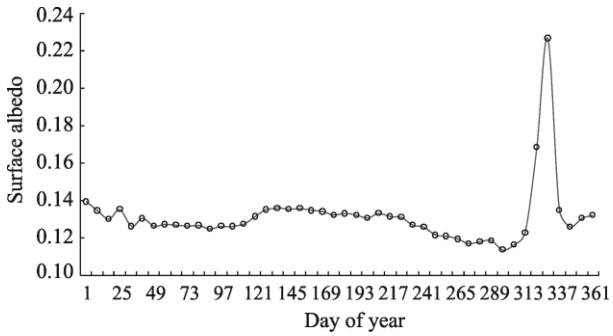

Fig. 4 Intra-annual variations in the surface albedo of Beijing, 2015.

Table 3 Seasonal averages of surface albedo in Beijing, 2015.

Seasons	Spring (day 30–120)	Summer (day 120–210)	Autumn (day 210–300)	Winter (day 300–30 of next year)
Mean	0.127	0.134	0.122	0.142
Standard deviation	0.001	0.002	0.006	0.030

3.2 Factors influencing albedo

3.2.1 Driving factor detection

Factor detector is a method to measure the relative importance of various factors for surface albedo. The greater the *q*-statistic of the factor detector, the greater is the influence of the respective explanatory factor on albedo. Moreover, the factor with the largest *q*-statistic is defined as the dominant factor. In this analysis, the response variable was taken as the annual average of the surface albedo of Beijing in 2015. According to the results of factor detection analysis (second row in Table 5), the degrees of influence of the six considered explanatory factors are ranked in the following order: NDVI (0.625) > LULC (0.537) > slope (0.531) > temperature (0.515) > elevation (0.512) > precipitation (0.190). All explanatory factors of surface albedo distribution passed the significance test ($P < 0.05$).

These explanatory factors all had significant individual effects on the spatial distribution of surface albedo values (Table 4). Among these different explanatory factors, the NDVI *q*-statistic is the largest, at is 0.625, indicating that this driving factor had the greatest influence overall. Therefore, NDVI is the dominant factor affecting surface albedo distribution in Beijing. LULC is the second-largest influence (*q*-statistic = 0.537); the influence of slope was less than that of LULC, which a *q*-statistic of 0.531; the average temperature and elevation had a similar level of influence (*q*-statistic = 0.515 and 0.512, respectively). These five factors all accounted for more than 50% of the surface albedo distribution. However, the *q*-statistic of cumulative precipitation is only 0.190, which is the smallest among all explanatory factors. That suggests the cumulative precipitation has only a minimal influence on the albedo distribution.

3.2.2 Ecological detection of explanatory factors

The ecological detector results are shown in Table 4. Y indicates that the influence of each explanatory factor on the spatial distribution of surface albedo is significantly different at the 95% confidence level, while N indicates that there is no significant difference.

The results show that there are no significant differences between the slope and the three other factors on surface albedo except for the NDVI and precipitation; and the influence of temperature and elevation were not significantly different. This shows that these factors have similar effects on the spatial distribution of surface albedo. The NDVI and cumulative precipitation each have a significantly different

influence than all other factors on the pattern of surface albedo; and other than for slope, LULC had significantly different influence compared to NDVI, elevation, temperature and precipitation. This shows that these factors play their respective roles in influencing the spatial distribution of surface albedo.

3.2.3 Interactive detection of explanatory factors

The spatial heterogeneity of surface albedo values results from multiple factors and there is often no single factor that can fully account for this variability. Interaction detector was used to assess whether the explanatory factors had an interactive influence on surface albedo. Based on the interaction detector results (Table 5), all of the considered explanatory factors were found to have a synergistic effect. This indicates that the combined influence of any two factors was greater than their individual effects. The *q*-statistic of the interactive influence between factors on surface albedo are ranked in the following order: NDVI ∩ LULC (0.710) > elevation ∩ NDVI (0.691) > slope ∩ NDVI (0.690) > temperature ∩ NDVI (0.689) > precipitation ∩ NDVI (0.648) > elevation ∩ LULC (0.645) > slope ∩ LULC (0.644) > temperature ∩ LULC (0.641) > temperature ∩ slope (0.630) > slope ∩ elevation (0.629) > precipitation ∩ LULC (0.573) > precipitation ∩ slope (0.567) > temperature ∩ elevation (0.553) > precipitation ∩ elevation (0.535) > precipitation ∩ temperature (0.531).

According to the results of the interaction detection, the *q*-statistic of the interaction between any two factors on the surface albedo is greater than the *q*-statistic for either of the two factors individual influences, but less than the sum of their *q* values, showing the bivariate enhancement results. Among them, NDVI and LULC had the largest interactive effect (0.710) while the combined effect of temperature and precipitation was lowest (0.531). The *q*-statistics of the four 2-factor combinations of NDVI ∩ LULC, elevation ∩ NDVI, slope ∩ NDVI and temperature ∩ NDVI are all greater than 0.680, indicating that these factors working together can explain more than 68% of the spatial distribution of surface albedo. The interaction of NDVI ∩ elevation is larger than that of NDVI ∩ slope or NDVI ∩ temperature, while the individual influence of elevation is smaller than that of slope or temperature. Similarly, the degree of interaction of elevation ∩ LULC was greater than between temperature ∩ LULC while the individual influence of elevation was lower than that of temperature. This indicates that NDVI has a greater enhancement of elevation than slope or temperature, and LULC enhanced the influence of elevation on surface albedo more than the temperature. It also indicates that a given factor may have different enhancement effects on the influence of different factors on surface albedo. In addition, while the influence of cumulative precipitation on the other factors was small, this factor cannot be ignored when its interactive effects are considered.

Table 4 Influence power index of the explanatory factors on the pattern of surface albedo in Beijing, 2015, and the significant differences between them.

Variables	LULC	NDVI	Elevation	Slope	Temperature	Precipitation
q-statistic	0.537	0.625	0.512	0.531	0.515	0.190
P value	0.000	0.000	0.000	0.000	0.000	0.000
LULC	–	–	–	–	–	–
NDVI	Y	–	–	–	–	–
Elevation	Y	Y	–	–	–	–
Slope	N	Y	N	–	–	–
Temperature	Y	Y	N	N	–	–
Precipitation	Y	Y	Y	Y	Y	–

Notes: Y indicates a significant difference between explanatory factors at the 95% confidence level; N indicates no significant difference.

Table 5 Interactions between explanatory factors in their influences of the spatial pattern of surface albedo in Beijing, 2015

Variables	LULC	NDVI	Elevation	Slope	Temperature	Precipitation
LULC	0.537					
NDVI	0.710*	0.625				
Elevation	0.645*	0.691*	0.512			
Slope	0.644*	0.690*	0.629*	0.531		
Temperature	0.641*	0.689*	0.553*	0.630*	0.515	
Precipitation	0.573*	0.648*	0.535*	0.567*	0.531*	0.190

Notes: * indicates that the interaction results in bivariate enhancement.

4 Discussion

4.1 Spatio-temporal heterogeneity of surface albedo

The spatio-temporal distribution of surface albedo in Beijing in 2015 was distinctly heterogeneous. The spatial variation of the average surface albedo in Beijing in 2015 was between 0.050 and 0.196. Higher albedo values were mainly distributed in the southeast of the city, which is densely populated, has a relatively flat topography, and is dominated by cropland and built-up land. In the northwest of the city, the terrain is higher and the main land-use types are grassland and forestland resulting in lower surface albedo values. Previous studies obtained the albedo of different surface features through remote sensing inversion, and the results were as follows: cropland > built-up land > grassland > forestland > unused land > water body (Bao et al., 2007). Bounoua et al. (2002) found that the surface albedo of forestland was significantly lower than that of cropland, because the color of the forestland canopy was generally darker than that of cropland, and the roughness of forestland was greater than that of cropland (Betts et al., 2007). The finding of these previous studies are consistent with the results of this study. In fact, even within the same type of land use, there are differences in surface albedo. This is because the surface albedo, as a quantitative index reflecting the reflective ability of the surface of earth to solar radiation, is not only related to the type of LULC, but it is also affected by other factors such as solar elevation angle, surface roughness, soil moisture and meteorological conditions (Chen, 1999; Liu et al., 2008; Guan et al., 2009). The factor detectors have also shown that LULC is only the dominant factor determining the change of surface albedo, not the only determinant. Therefore, when a given land use type is located in different regions, its climatic conditions, soil types and solar radiation received are very different, resulting in differences in surface albedo.

In 2015, the temporal variation of the overall mean surface albedo across the entire city was between 0.114 and 0.227, with a mean of 0.131. This variation reflected significant seasonal patterns, with higher and more fluctuating values occurring in the winter, relatively stable values occurring in the summer and spring, and a slight decline in values in the autumn. Snow and ice have a high albedo to solar radiation, only a small part of the incoming solar radiation energy is absorbed by the snow-and ice-covered areas. The melting of snow will expose the surface that will significantly reduce the surface albedo (Nolin et al., 1997; Robinson, 1997). So the large variation of surface albedo during the winter is probably due to the snow. These annual changes of albedo are consistent with existing research results (Yang et al., 2006). The spatio-temporal results of this study help to understand the temporal and spatial variability of Beijing's surface albedo and provided a powerful reference for the simulation of environmental climate change.

4.2 Relative influences of factors on surface albedo

According to the analysis results of the factor detector, all each of the factors considered in this study show a significant relationship with the spatial heterogeneity of surface albedo. Among these, NDVI had the highest *q*-statistic value of 0.625, indicating it had the greatest level of influence. Previous studies have also shown that NDVI has a strong negative correlation with the surface albedo (Xue et al., 2019). This is because NDVI reflects the type of land cover, and the change of land cover type directly leads to the difference of land cover albedo (Li et al., 2012). However, in the summer with high NDVI, the surface albedo of Beijing is even higher than in spring and autumn when NDVI is low, which also indicates that NDVI is only the dominant factor determining the spatial distribution of surface albedo, not the only determinant. The fact that surface albedo increases in summer in Beijing indicates that the decrease of the surface albedo caused by NDVI is less than the increase of the surface albedo caused by other factors. LULC is second only to NDVI in influencing the spatial distribution of surface albedo, with a *q*-statistic of 0.537. This is consistent with the results of previous studies which have also shown that surface albedo is strongly correlated with land use and land-cover type (Zhou et al., 2003; Liu et al., 2015). That correlation is mainly due to the different surface properties of ground objects, which have distinct reflective characteristics with respect to solar radiation (Zhang, 2008). In addition, the *q*-statistics of slope, elevation, and average temperature were all above 0.500 indicating that they also had large influences on surface albedo. In comparison, the effect of cumulative precipitation was low with a *q*-statistic of 0.190, indicating it does not play a dominant role in surface albedo. Some studies based on classical statistics can only show a good correlation between surface albedo and precipitation but cannot indicate how much influence it has (Wang et al., 2011). The geographical detector approach has no linear hypothesis, so the relationship between dependent variables and independent variables is, as such, more reliable than that obtained by classical statistics. It judges the influence of independent variables on the spatial differentiation of dependent variables using the *q*-statistic, whereby independent variable *X* explains the dependent variable *Y* as *q*, which is also an advantage of the geographical detector over classical statistical methods. Comparing the spatial distribution maps of the six factors considered with surface albedo, the greatest degree of similarity can be seen between surface albedo and LULC, NDVI, slope, elevation, and temperature. This conforms to the core premise of the geographical detectors approach, that the spatial distribution of a dependent variable should be similar to an independent variable if they are significantly associated with each other (Wang et al., 2010; Wang et al., 2016).

The ecological detector results show that some factors

are significantly different from other variables in terms of their effects on the spatial distribution of surface albedo. For example, there are significant differences between cumulative precipitation and other factors in influencing the spatial distribution of albedo. These differences also show that some factors play their respective roles in influencing the distribution of the albedo. The results of the interactive detector show that there is interaction between all variables, indicating that the spatial heterogeneity of surface albedo is the result of multiple factors. The results also show that the interaction of any two factors will enhance the driving force for albedo spatial differentiation. However, the driving force of the two variables acting together is not simply the sum of the driving forces of the two variables acting independently. Different variables have different enhancement effects when interacting with each other and any given variable has different enhancement effects on other variables. The interaction detector can not only judge whether there is variable interaction or not, but it can also judge the strength, direction, linearity or nonlinearity of the interaction (Wang et al., 2010). Therefore, it is useful for studying the interactions between variables.

Admittedly, only some of the factors influencing surface albedo were quantitatively analysed in this study. In addition to the factors considered here, previous studies have shown that solar height angle, atmospheric composition, surface roughness, and snow cover also have important influences on surface albedo (Davidson and Wang, 2005; Wang, 2005). In addition, this study only used the average surface albedo of Beijing in 2015 to quantitatively analyse the driving forces of various factors on the spatial heterogeneity of the surface albedo, which lacked the consideration of the time changes of the driving forces. In the follow-up work, we analysed the change of the *q*-statistic between the explanatory variable and surface albedo with the changes of time and space. Studies have shown that the main factors affecting the albedo of temperate grassland surfaces are different in different periods (Wang and Davidson, 2007). Therefore, the influence of other possible factors on the spatial distribution of surface albedo and their variability over time in urban areas such as Beijing require further research.

5 Conclusions

This study used GLASS surface albedo data to study the spatial and temporal distribution of surface albedo in Beijing in 2015. Combined with LULC, NDVI, elevation, slope, average temperature, and cumulative precipitation data, the degree of influence of these factors on albedo was studied by using the geographical detector approach. The results show that:

(1) The annual average albedo in Beijing ranged between 0.050 and 0.196, and there were significant spatial differences with higher values in the southeast and lower values in the northwest of the city. Across the year, the spatially averaged albedo varied between 0.114 and 0.227, with an annual mean of 0.131. Albedo was relatively stable during the spring, peaked at 0.227 during the winter, and reached its lowest value of 0.114 in the autumn.

(2) The factor detector analysis showed that each of the considered factors had a significant influence on the spatial heterogeneity of surface albedo, with their effects being ranked based on their *q*-statistics in the following descending order: NDVI (0.625) > LULC (0.537) > slope (0.531) > temperature (0.515) > elevation (0.512) > precipitation (0.190). As such, NDVI had the greatest influence on the spatial heterogeneity of surface albedo in 2015 and precipitation had the smallest influence.

(3) The relative influences of the explanatory factors on the spatial distribution of surface albedo varied significantly. For example, both NDVI and precipitation are significantly different from all the other factors. Except for slope, LULC also had a significantly different effect than the other factors. However, interactions occurred among all of the factors, with the combination of any two explanatory factors having an enhanced effect on surface albedo; the effects of these interactions were additive. LULC and NDVI had the strongest interactive effect, with a combined *q*-statistic of 0.710, while the interactive effect between temperature and precipitation was weakest, with a combined *q*-statistic of 0.531. Overall, these findings demonstrate that the observed spatial and temporal patterns of albedo were the result of multiple, interacting factors.

References

Bao P Y, Zhang Y J, Gong L, et al. 2007. Study on consistency of land surface albedo obtained from ETM+ and MODIS. *Journal of Hohai University* (*Natural Sciences*), 35(1): 67–71. (in Chinese).

Betts A K, Desjardins R L, Worth D. 2007. Impact of agriculture, forest and cloud feedback on the surface energy budget in BOREAS. *Agricultural and Forest Meteorology*, 142(2–4): 156–169.

Bounoua L, Defries R, Collatz G J, et al. 2002. Effects of land cover conversion on surface climate. *Climatic Change*, 52(1–2): 29–64.

Cao F, Ge Y, Wang J F. 2013. Optimal discretization for Geographical Detectors-based risk assessment. *Giscience & Remote Sensing*, 50(1): 78–92.

Chen X H. 1999. Relationship between surface albedo and some meteorological factors. *Journal of Chengdu Institute of Meteorology*, 14(3): 233–238. (in Chinese)

Chu L, Huang C, Liu Q S, et al. 2019. Spatial heterogeneity of winter wheat yield and its determinants in the Yellow River Delta, China. *Sustainability*, 12(1): 135. DOI: 10.3390/su12010135.

Davidson A, Wang S S. 2005. Spatiotemporal variations in land surface albedo across Canada from MODIS observations. *Canadian Journal of Remote Sensing*, 31(5): 377–390.

Dickinson R E. 1983. Land surface processes and climate—Surface albedos and energy balance. *Advances in Geophysics*, 25: 305–353.

Ding Y T, Zhang M, Qian X Y, et al. 2019. Using the geographical detector technique to explore the impact of socioeconomic factors on $PM_{2.5}$ concentrations in China. *Journal of Cleaner Production*, 211: 1480–1490.

Golkar F, Sabziparvar A A, Khanbilvardi R, et al. 2018. Estimation of in-

stantaneous air temperature using remote sensing data. *International Journal of Remote Sensing*, 39(1): 258–275.

Govaerts Y, Lattanzio A. 2008. Estimation of surface albedo increase during the eighties Sahel drought from Meteosat observations. *Global and Planetary Change*, 64(3–4): 139–145.

Guan X D, Huang J P, Guo N, et al. 2009. Variability of soil moisture and its relationship with surface albedo and soil thermal parameters over the Loess Plateau. *Advances in Atmospheric Sciences*, 26(4): 692–700.

He T, Liang S L, Song D X. 2014. Analysis of global land surface albedo climatology and spatial-temporal variation during 1981–2010 from multiple satellite products. *Journal of Geophysical Research*: *Atmospheres*, 119(17): 10281–10298.

Hu Y, Wang J F, Li X H, et al. 2011. Geographical Detector-based risk assessment of the under-five mortality in the 2008 Wenchuan Earthquake, China. *Plos One*, 6(6): 1–8.

Li H F, Yuan Z L, Yu T, et al. 2012. Surface albedo estimating based on HJ-1/CCD and relationship analysis between albedo and NDVI. *Remote Sensing Information*, 27(4): 16–21. (in Chinese).

Liao Y L, Wang J F, Wu J L, et al. 2010. Spatial analysis of neural tube defects in a rural coal mining area. *International Journal of Environmental Health Research*, 20(6): 439–450.

Liu H Z, Wang B M, Fu C B. 2008. Relationships between surface albedo, soil thermal parameters and soil moisture in the semi-arid area of Tongyu, northeastern China. *Advances in Atmospheric Sciences*, 25(5): 757–764.

Liu J Y, Kuang W H, Zhang Z X, et al. 2014. Spatiotemporal characteristics, patterns, and causes of land-use changes in China since the late 1980s. *Journal of Geographical Sciences*, 24(2): 195–210.

Liu N F, Liu Q, Wang L Z, et al. 2013a. A statistics-based temporal filter algorithm to map spatiotemporally continuous shortwave albedo from MODIS data. *Hydrology and Earth System Sciences*, 17(6): 2121–2129.

Liu Q Q, Cui Y P, Liu S J, et al. 2019. Study on surface albedo of spectral radiation of different land use types in China. *Remote Sensing Technology and Application*, 34(1): 45–56. (in Chinese).

Liu Q, Wang L Z, Qu Y, et al. 2013b. Preliminary evaluation of the long-term GLASS albedo product. *International Journal of Digital Earth*, 6(S1): 69–95.

Liu Z J, Shao Q Q, Tao J, et al. 2015. Intra-annual variability of satellite observed surface albedo associated with typical land cover types in China. *Journal of Geographical Sciences*, 25(1): 35–44.

Loarie S R, Lobell D B, Asner G P, et al. 2011. Direct impacts on local climate of sugar-cane expansion in Brazil. *Nature Climate Change*, 1(2): 105–109.

Lou C R, Liu H Y, Li Y F, et al. 2016. Socioeconomic drivers of $PM_{2.5}$ in the accumulation phase of air pollution episodes in the Yangtze River Delta of China. *International Journal of Environmental Research and Public Health*, 13(10): 1–19.

Malahlela O E, Adjorlolo C, Olwoch J M, et al. 2019. Integrating geostatistics and remote sensing for mapping the spatial distribution of cattle hoofprints in relation to malaria vector control. *International Journal of Remote Sensing*, 40(15): 5917–5937.

Nikolaos B, Nektarios C. 2015. Estimation of the land surface albedo changes in the Broader Mediterranean Area, based on 12 years of satellite observations. *Remote Sensing*, 7(12): 16150–16163.

Nolin A W, Stroeve J. 1997. The changing albedo of the Greenland ice sheet: Implications for climate modeling. *Annals of Glaciology*, 25: 51–57.

Qu Y, Liu Q, Liang S L, et al. 2014. Direct-estimation algorithm for mapping daily land-surface broadband albedo from MODIS data. *IEEE Transactions on Geoscience and Remote Sensing*, 52(2): 907–919.

Ranson K J, Irons J R, Daughtry C S T. 1991. Surface albedo from bidirectional reflectance. *Remote Sensing of Environment*, 35(2–3): 201–211.

Richardson A D, Keenan T F, Migliavacca M, et al. 2013. Climate change, phenology, and phenological control of vegetation feedbacks to the climate system. *Agricultural and Forest Meteorology*, 169: 156–173.

Robinson D A. 1997. Hemispheric snow cover and surface albedo for model validation. *Annals of Glaciology*, 25: 241–245.

Russell M J, Nunez M, Chladil M A, et al. 1997. Conversion of nadir, narrowband reflectance in red and near-infrared channels to hemispherical surface albedo. *Remote Sensing of Environment*, 61(1): 16–23.

Schaaf C B, Gao F, Strahler A H, et al. 2002. First operational BRDF, albedo nadir reflectance products from MODIS. *Remote Sensing of Environment*, 83(1–2): 135–148.

Wang G, Han L, Ji X J. 2011. Research of the reason for variations of surface albedo in different areas in China from 1982 to 1998. *Journal Chongqing University Technology* (*Nature Science*), 28(4): 79–83. (in Chinese)

Wang J F, Hu Y. 2012. Environmental health risk detection with GeogDetector. *Environmental Modelling & Software*, 33: 114–115.

Wang J F, Li X H, Christakos G, et al. 2010. Geographical detectors-based health risk assessment and its application in the neural tube defects study of the Heshun Region, China. *International Journal of Geographical Information Science*, 24(1): 107–127.

Wang J F, Zhang T L, Fu B J. 2016. A measure of spatial stratified heterogeneity. *Ecological Indicators*, 67: 250–256.

Wang L Z, Chen L J. 2018. The impact of new transportation modes on population distribution in Jing-Jin-Ji region of China. *Scientific Data*, 5: 170204. DOI: 10.1038/sdata.2017.204

Wang S S, Davidson A. 2007. Impact of climate variations on surface albedo of a temperate grassland. *Agricultural and Forest Meteorology*, 142(2–4): 133–142.

Wang S S. 2005. Dynamics of surface albedo of a boreal forest and its simulation. *Ecological Modelling*, 183(4): 477–494.

Wang Z B, Liang L W, Sun Z, et al. 2019. Spatiotemporal differentiation and the factors influencing urbanization and ecological environment synergistic effects within the Beijing-Tianjin-Hebei urban agglomeration. *Journal of Environmental Management*, 243: 227–239.

Xiao D, Tao F, Moiwo J P. 2011. Research progress on surface albedo under global change. *Advances in Earth Science*, 26(11): 1217–1224.

Xue H Z, Zhang G D, Zhou H M, et al. 2019 Time series variation characteristics and parameterization of land surface albedo in several typical land cover types. *Journal of Beijing Normal University* (*Natural Science*), 55(2): 272–283. (in Chinese).

Yan Y C, Ju H R, Zhang S R, et al. 2019. Spatiotemporal patterns and driving forces of urban expansion in coastal areas: A study on urban agglomeration in the Pearl River Delta, China. *Sustainability*, 12(1): 191. DOI: 10.3390/su12010191

Yang J Q, Li Z, Zhai P, et al. 2020. The influence of soil moisture and solar altitude on surface spectral albedo in arid area. *Environmental Research Letters*, 15(3): 1–10.

Yang J, Chen H B, Wang K C, et al. 2006. Analysis of the surface albedo distribution and variation in Beijing region by using the MODIS data. *Remote Sening Technology and Application*, 21(5): 503–506. (in Chinese).

Yang W T, Deng M, Xu F, et al. 2018. Prediction of hourly $PM_{2.5}$ using a space-time support vector regression model. *Atmospheric Environment*, 181: 12–19.

Yuan L H, Chen X Q, Wang X Y, et al. 2019. Spatial associations between NDVI and environmental factors in the Heihe River Basin. *Journal of Geographical Sciences*, 29(9): 1548–1564.

Zhang X T, Liang S L, Wang K C, et al. 2010. Analysis of global land surface shortwave broadband albedo from multiple data sources. *IEEE*

Journal of Selected Topics in Applied Earth Observations and Remote Sensing, 3(3): 296–305.

Zhang Y H, Lu H P, Qu W C. 2020. Geographical detection of traffic accidents spatial stratified heterogeneity and influence factors. *International Journal of Environmental Research and Public Health*, 17(2): 572. DOI: 10.3390/ijerph17020572.

Zhang Y M. 2008. Spectrum characteristics of surface features reflection and high spectral imaging remote sensing. *Electro-Optic Technology Application*, 23(5): 6–11.

Zhou C, Zhu N N, Xu J H, et al. 2019. The contribution rate of driving factors and their interactions to temperature in the Yangtze River Delta region. *Atmosphere*, 11(1): 32. DOI: 10.3390/atmos11010032.

Zhou L, Dickinson R E, Tian Y, et al. 2003. Comparison of seasonal and spatial variations of albedos from Moderate-Resolution Imaging Spectroradiometer (MODIS) and Common Land Model. *Journal of Geophysical Research*: *Atmospheres*, 108(D15): 4488. DOi: 10.1029/2002JD003326.

基于地理探测器的北京市地表反照率时空分异及其驱动因素研究

刘亲亲[1,2]，田亦陈[2]，尹　锴[2]，张飞飞[2]，袁　超[2]，杨　光[2]

1. 中国科学院大学，北京 100049；
2. 中国科学院空天信息创新研究院，北京 100101

摘　要：地表反照率直接影响着辐射平衡和地表热收支，是地球-大气系统研究中的关键因子。本文研究了 2015 年北京市地表反照率的时空分布特征，并基于地理探测器定量分析了地表反照率空间分异的驱动因素及其交互作用。结果表明：北京市地表反照率呈东南高、西北低的趋势；冬季变化最大，春季变化最小；年地表反照率最小值出现在秋季，最大值出现在冬季，具有显著的时空异质性。土地覆盖类型、NDVI、高程、坡度、温度和降水对地表反照率的空间分异均有显著影响，影响力分别为 0.537、0.625、0.512、0.531、0.515 和 0.190；且一些驱动因素对反照率空间分布的影响存在显著差异。任意两种驱动因素之间均存在交互作用，表现出双变量增强的结果。其中，地表覆盖类型与 NDVI 的交互作用最大，影响力为 0.710，而温度与降水的交互作用最弱，影响力为 0.531。研究结果为了解北京市地表反照率的时空分布特征以及区域气候和陆面模式中能量模块的物理过程提供了科学依据。

关键词：地表反照率；时空分布；解释因子；地理探测器